Combining a transcriptomic approach and a targeted metabolomics approach for deciphering the molecular bases of compatibility phenotype in the snail Biomphalaria glabrata toward Schistosoma mansoni.

Elodie Simphor, Anne Rognon, Emmanuel Vignal, Sylvain Henry, Jean-François Allienne, Andrei Turtoi, Cristian Chaparro, Richard Galinier, David Duval, Benjamin Gourbal

Acta Tropica 2024

Combining a transcriptomic approach and a targeted metabolomics approach for deciphering the molecular bases of compatibility phenotype in the snail *Biomphalaria glabrata* toward *Schistosoma mansoni*.

Elodie Simphor[1], Anne Rognon [1], Emmanuel Vignal[1], Sylvain Henry[2], Jean-François Allienne[1], Andrei Turtoi[2,3], Cristian Chaparro[1], Richard Galinier[1], David Duval[1] and Benjamin Gourbal[1, $]

[1] IHPE, Univ. Montpellier, CNRS, Ifremer, Univ. Perpignan via Domitia, Perpignan, France.

[2] Platform for Translational Oncometabolomics, Biocampus, CNRS, INSERM, Université de Montpellier, Montpellier, France.

[3] Tumor Microenvironment and Resistance to Therapy Laboratory, Institut de Recherche en Cancérologie de Montpellier, Université de Montpellier, INSERM U1194, Montpellier, France

Bullet points :

- Molecular support of *S. mansoni / B. glabrata* compatibility
- Non-clonal snail lines with same genetic background.
- 328 genes differentially regulated in resistant vs susceptible phenotypes.
- Lipid compounds modulated in resistant vs susceptible phenotypes.

Corresponding authors:

Pr. Benjamin Gourbal: Benjamin.gourbal@univ-perp.fr

IHPE laboratory, 58 avenue Paul Alduy 66860 Perpignan France

Tel (+33) 4 68 66 21 88

Abstract

Biomphalaria glabrata is a freshwater snail and the obligatory intermediate host of *Schistosoma mansoni* parasite, the etiologic agent of intestinal Schistosomiasis, in South America and Caribbean. Interestingly in such host-parasite interactions, compatibility varies between populations, strains or individuals. This observed compatibility polymorphism is based on a complex molecular-matching-phenotype, the molecular bases of which have been investigated in numerous studies, notably by comparing between different strains or geographical isolates or clonal selected snail lines. Herein we propose to decipher the constitutive molecular support of this interaction in selected non-clonal resistant and susceptible snail strain originating from the same natural population from Brazil and thus having the same genetic background. Thanks to a global RNAseq transcriptomic approach on whole snail, we identified a total of 328 differentially expressed genes between resistant and susceptible phenotypes among which 129 were up-regulated and 199 down-regulated. Metabolomic studies were used to corroborate the RNAseq results. The activation of immune genes and specific metabolic pathways in resistant snails might provide them with the capacity to better respond to parasite infection.

Keywords: *Biomphalaria glabrata; Schistosoma mansoni*; resistance/susceptibility; RNAseq lipid metabolism pathway

1 Introduction

Schistosomes are the causative agents of schistosomiasis disease, which is one of the most important human tropical neglected parasitic diseases in the world after malaria. Schistosomes infect over 200 million people worldwide, causing both acute and chronic debilitating diseases (Alwan et al., 2023). There is no effective vaccine against schistosomes, and the treatment of schistosomiasis still relies on a single drug called praziquantel (Doenhoff et al., 2009; Zhu et al., 2023). However, praziquantel has limitations in killing juvenile worms (schistosomula) and their extensive use in mass drug administration has been linked to the emergence of parasite drug resistance (Alonso et al., 2006; Couto et al., 2011; Fallon and Doenhoff, 1994; Gryseels et al., 1994; William et al., 1999). To overcome some of these praziquantel limitations new strategies are urgently needed to control schistosomiasis. To accomplish its life-cycle, schistosome parasites need a fresh water snail as intermediate host. In the snail, the parasite undergoes an intense asexual multiplication to enhance its transmission in the water environment through the shedding of cercariae, the parasite stage known to infect the human definitive host. Only freshwater snails are able to transmit the parasite, thus, breaking parasite transmission through its intermediate snail host, as recommended by the World Health Organization, may represent a truly relevant strategy (Famakinde, 2018).

In South America, the freshwater snail, *Biomphalaria glabrata* (*B. glabrata*) is the main snail susceptible to an infection by the trematode worm *Schistosoma mansoni (S. mansoni)*. However, within a same snail species, compatibility varies between populations, strains or individuals (Basch, 1975; Mitta et al., 2017; Theron and Combes, 1995). Snail/schistosome compatibility reflects both snail susceptibility and schistosome infectivity and the observed polymorphism of compatibility results from the complex phenotype-by-phenotype interactions occurring between each individual host and each individual parasite (Galinier et al., 2017; Mitta et al., 2017). Therefore, deciphering the complex molecular dialogue occurring between the host and the parasite would help in identifying new potential strategies to fight and control the disease. This observed compatibility polymorphism is based on a complex molecular-matching-phenotype (Mitta et al., 2017). The molecular bases of such compatibility polymorphism have been investigated in the past by (i) comparing different parasite

geographic isolates against the same snail host (Roger et al., 2008), (ii) comparing two strains of snail against the same parasite isolate (Roger et al., 2008), (iii) doing multiple sympatric and allopatric comparisons between different strains or geographic isolates of hosts and parasites (Mitta et al., 2017) or finally (iv) by comparing clonally selected snail lines of segregated phenotypes of resistance and susceptibility (Allan et al., 2018, 2017; Mulvey and Woodruff, 1985; Tennessen et al., 2015b, 2015a). All these approaches have yielded a significant number of important results on the molecular mechanisms involved in snail/schistosome compatibility. Notwithstanding, a few biases exist concerning those studies. In the studies mentioned in (i), (ii) and (iii), the authors compared different genetic backgrounds for different strains or geographical isolates with totally different evolution or co-evolution histories. Second, for point (iv), the authors investigated clonal lines of snails and parasites which exhibit reduced or no genetic diversity that may compromise the identification of the overall complexity of compatibility mechanisms. Herein, we propose a new approach to decipher the constitutive molecular support of snail/schistosome interaction in selected but non-clonal snail strains originated from the same snail species with the same genetic background and evolutionary history. From a *B. glabrata* snail population originating from Brazil, more precisely the locality of Barreiro (BgBAR2), we selected two snail strains, one resistant and the other susceptible to *S. mansoni* Venezuela (SmVEN). Those two phenotypes were segregated over 5 generations, from a original field isolate with a prevalence of 78%, cross breeding at each generation were conducted in order to maintain the genetic diversity of the selected strains. Finally, the constitutive molecular differences between resistant and susceptible phenotypes were investigated using a combination of omics approaches on whole snails. We believe that this novel approach might be helpful to decipher more precisely the molecular processes at play at the core of snail/schistosome interactions.

2 Materials and Methods

2.1 Ethics statement

Our laboratory holds permit #39910-2022121915564694 (APAFIS number) for experiments on animals from the French Ministry of Agriculture and Fisheries and the DDPP Languedoc-Roussillon (Direction Départementale de Protection des Populations) Montpellier, France

(authorization # 007083) and the Ethic committee CEEA-LR (# C66-136-01). The housing, breeding, and animal care of the utilized animals followed the ethical requirements of our country. The researchers also possess an official certificate for animal experimentation (Decree # 87–848, October 19, 1987). Animal experimentation followed the guidelines of the French CNRS.

2.2 Biological model, phenotype selection and experimental infection procedures

All the experimental approaches conducted in the present study were executed with the freshwater snail *B. glabrata* originating from Barreiro Brazil (named BgBAR2) experimentally infected with the trematode parasite *S. mansoni* recovered from Venezuela (named SmVen) (Theron et al., 2014). During 5 generations, snails were subjected to parasite infection and offspring originating from infected snails were kept to start a susceptible population and offspring from non-infected snails were kept for constituting a resistant population of snails, then, cross breeding were done for each generation and each population to avoid loss of genetic diversity. The susceptible phenotype had 95% prevalence (named BgBAR2S) and the resistant phenotype had 6% prevalence (named BgBAR2R). Since 2019, the phenotypes are perfectly stable in our laboratory conditions without the necessity to maintain the parasite infection pressure. Then, a combination of omics approaches (transcriptomic and metabolomics) has been conducted to investigate constitutive differences between resistant and susceptible phenotypes on whole snails.

2.3 Biological samples, RNA extraction and sequencing

Four pools of 10 resistant snails (R1 to R4) and four pools of 10 susceptible snails (S1 to S4) were prepared. For each pools, the snails were selected from different classes of size to approximate different ages (control for age effect) in the population as follow: 2 snails from 11 to 13 mm (age : 18 to 20 weeks), 2 from 9-11 mm (age : 13 to 15 weeks), 3 from 7 to 9 mm (age : 10 to 13 weeks) and 3 from 5 to 7 mm (age : 8 to 10 weeks). Before sampling, snails were fasting during 48 hours. Then snails were removed from their shell before pooling and were ground in liquid nitrogen. RNA was extracted using Trizol reagents (Invitrogen) according to manufacturer instructions. Samples were quantified using Qubit 2.0 fluorimeter and stored at -80°C until use. For each sample, -1 µg of RNA was used for sequencing using Illumina NextSeq

in single-end reads of 75 pb with polyA+ RNAseq librairies, in order to obtain approximately 25 million reads per sample. Samples were prepared using NEBNext Ultrall Directional RNAseq libraries, followed by quality control using the 2100 Bioanalyzer instrument (Agilent) and sequencing using NextSeq550 Flow Cell high Output SR75.

2.4 RNA sequencing bioinformatics processing

The read quality of each replicate sample (R1, R2, R3, R4 and S1, S2, S3, S4) fastq file was assessed with the FASTQC tool version 0.11.8 (phred score > 30 for all bases and GC percentage of 50%). Reads were trimmed using Trim-galore tool (version 0.6.3) with the following parameters of each single-end library: -automatic detection of sequence adapters, phred score threshold > 30, overlap with the adaptor sequence set to 1, maximum allowable error rate of 0.1, rejection of reads shorter than 20 base pairs. Reads were mapped with the RNA-STAR tool (version 2.7.8a) (Dobin et al., 2013) on the *Biomphalaria glabrata* reference genome BB02 (version 1.7 available on Vector base: https://vectorbase.org/vectorbase /app). Mapping with the STAR tool, for differential expression analysis was focus on protein coding genes, with genome annotation file (version 3 available on vector base), average mapping of 96 % was obtained for susceptible and resistant replicates (Table S1).

Read count was done using htseq-count tool using union mode. The threshold for alignment quality was set at a minimum of 10 base pairs. Differential analysis of gene expression was performed in R using the DEseq2 (package version 1.37.5) (Love et al., 2014). We also normalized our reads in TPM (transcripts per million) in Table S2 (Vera Alvarez et al., 2019; Zhao et al., 2021).

The *B. glabrata* BB02 genome (Genbank GCA_000457365.1, VectorBase rel. 49, 2020-NOV-05) was used as a reference. We conducted a re-annotation of the genome that has been named IHPE lab annotation, to enhance the *B. glabrata* gene annotation of the BB02 genome (see table S2 and S8). Prior to re-annotation, the longest CDS sequences were extracted from the gff3 file. Then, new annotation was performed using the ORSON script (https://gitlab.ifremer.fr/bioinfo/workflows/orson). ORSON combines state-of-the-art tools for annotation processes within a Nextflow pipeline. ORSON script performs sequence similarity search with BLAST (Altschul et al., 1990), functional prediction with InterProScan

(Jones et al., 2014) and eggNOG (Huerta-Cepas et al., 2019) orthogroup annotation. Interproscan analysis was performed against Pfam, Prosite, CDD, TIGR, SMART, SuperFamily, PRINTS and Hamap databases. Results were collected and processed using Blast2GO (Götz et al., 2008) for annotation mapping and validation.

2.5 Gene ontology enrichment analysis

Functional enrichment and identification of metabolic pathways were performed on the 328 DEGs using Rank-Based Gene Ontology Analysis with Adaptative Clustering (RBGOA) (https://github.com/z0on/GO_MWU) and String DB VERSION 11.5 (https://string-db.org/). In RBGOA (Wright et al., 2015) a corrected p-value of 0.01 was considered for over-expressed and down-regulated genes.

We selected GO terms with a p-value < 0.01 Mann-Whitney U (MWU). The visualization of selected Gene Ontology (GO) terms using RBGOA was conducted with the REVIGO software (http://revigo.irb.hr/) (Table S3 and S4).

KEGG pathways were analysed using STRING DB platform (Szklarczyk et al., 2023). The protein sequences of the 328 DEGs and the organism name *Biomphalaria glabrata* were provided as input. STRING database confirmed and predicted connections between proteins, encompassing physical interactions as well as functional associations. STRING basic input parameters were selected (full STRING) network; all interactive sources; medium confidence set to 0.400; and the maximum number of interactors was set to 50. Based on these settings 57 genes over the 328 DEGs were associated to a KEGG pathways (Table S5).

2.6 Lipidomics analysis and bioinformatics

Six replicates for resistant (R1 to R6) and susceptible (S1 to S6) snail-pools were prepared (3 snails/pool/replicate, snail size 7-9 mm). Resistant and susceptible snails were maintained in the same tank, fasted, for 48 hours prior to sampling. Then, for each replicate, 3 snails were removed from their shells and weighed to prepare 100 mg of total snail tissue. Each sample was ground in liquid nitrogen and stored at -80°C until use.

Extraction solvent made of chloroform (cat. No. 438681, Carlo Erba, Emmendingen, Germany) /methanol (cat. No. 0013684102BS, Biosolve, Valkenswaard, The Netherlands) mixture (2:1 v/v) was prepared and pre-cooled to -20°C for 2h prior to use. To each sample, 1 mL of the pre-cooled extraction solvent and 10 µL of the internal standards mix (cat. 330710X-1 EA, Sigma Aldrich, St. Louis, MO, USA) were added to the 100 mg of snail tissue. The samples were vortexed for 10 s, then placed at 4°C and subjected to continuous rotation for 30 minutes. Following this, 200 µL of ice cold 5% acetic acid were added to the samples. The samples were then vortexed for 10 seconds and incubated at -20 °C for 2 hours. Next, the samples were centrifuged at 15 000 g for 20 minutes at 4 °C. The lower phase of the resulting mixture was carefully transferred to a 1.5 mL Eppendorf tube. The lower phase was subjected to drying using a speedvac system. Finally, the dried samples were reconstituted in 1 mL of a pre-cooled (-20 °C) mixture consisting of isopropanol and methanol (2:1 v/v).

Chromatographic analysis was performed using UHPLC 1290 Infinity II with an ZORBAX Eclipse Plus C18 100 x 2.1 mm, 1.8 µm, column (Agilent, Santa Clara, CA, USA). The mobile phase A consisted of a 5:3:2 mix of 10 mM ammonium formate (cat. No. 70221, Sigma Aldrich), 5 µM Agilent deactivator additive (cat. No. 5191-3940, Agilent) in water (cat. No. 0023214102BS, Biosolve), acetonitrile (cat. No. 0001207802BS, Biosolve) and 2-propanol (cat. No. 33539 Honeywell, Charlotte, NC, USA). Mobile phase B was a 1:9:90 mix of 10 mM ammonium formate in water, acetonitrile, 2-propanol. The gradient used was: 15% B, 0 minute; 50% B, 2.50 minutes; 57% B, 2.60 minutes; 70% B, 9.00 minutes; 93% B, 9.10 minutes; 96% B, 11.00 minutes; 100% B, 11.10 minutes; 100% B, 16.00 minutes; 15% B, 16.20 minutes, 15% B, 20 minutes. The column temperature was set to 45 °C, flow rate 0.4 mL/min, and volume of injection to 0.5 µL for each run. Lipidomic profiling analysis was performed on a 6495 LC/TQ mass system and the Agilent MassHunter workstation with the dynamic MRM scan mode. Source-parameter settings in the positive or negative modes were as follows: i) the capillary voltage was set at 3.5 kV for positive mode and 3 kV for negative mode, ii) gas temperature at 150°C and gas flow at 17 L/min, iii) nebulizer at 20 psi, iv) sheath gas temperature at 200 °C and v) sheath gas flow at 10 L/min. Further details on the selected MRMs were described

Following the data acquisition, the chromatographic data were first imported into Agilent MassHunter Quantitative Analysis (for QQQ) where integration window for all identified compounds was individually defined using the “spectrum summation” integration algorithm

available in the software. Prior to normalization, the area subtraction (sample - blank) for each compound present in the blank was performed. Normalization was calculated by dividing the peak area of the analyte by that of its respective internal standard. Internal standards are consist of stable-isotope-labeled and nonphysiological species that are chromatographically close to a given group of lipids (for further details refer to Huynh et al., 2019). The data were then imported in R (4.0.2) (R Core Team, 2021). Outliers among the samples were identified using the Grubbs's test (R package "outliers") and samples S6 and R1 were removed from the analysis as they have been identified as outliers. The data where further analyzed using the MetaboAnalyst package (4.0) (Chong et al., 2019). Following the creation of the MetaboAnalyst object, the data were scaled using the "AutoNorm" argument within the "Normalization" function. Scaled data were then evaluated using partial least squares discriminant analysis (PLS-DA) and correlation analysis with "PLSR.Anal" and "FeatureCorrelation" functions respectively. The code used for the analysis can be found here: https://github.com/DirtyHarry80/PUFAMetaboR.

2.7 Adenosine Tri-Phosphate (ATP) quantification in susceptible and resistant snails

Seven biological replicates for susceptible and resistant snails were used (126 snails, 7-9 mm size). Snails were removed from their shell and for each replicate, 9 snails were weighed to prepare. 300 mg of tissue, which were grounded in liquid nitrogen. 1 mL of ice-cold homogenisation buffer (HEPES-NaOH) was homogenized with 100 µL of 0.1 mm diameter glass beads in a MagNA Lyser (Roche) apparatus and perform 3 runs of 15 seconds at 7000 rpm. Samples were then centrifuged at 1000 g for 10 minutes at 4°C. 300 µL of supernatant were recovered and complemented with 300 µL of ice-cold 10% TCA (V/V) and finally centrifuged at 10 000 g for 10 minutes at 4°C, 400 µL of the supernatant were mixed with 200 µL of neutralization buffer (Chida et al., 2012). ATP determination was conducted according to the instructions of the ATP Determination kit from Invitrogen. Briefly, the concentration of ATP in each sample is determined using a standard curve of ATP obtained with firefly luciferase from 1 nM to 1 µM. Bioluminescence was measured using a luminometer at a wavelength of 560 nm. Statistical analyses were done using a Mann-Whitney U test (p-value considered significant at $p < 0.05$).

3 Results

3.1 Differentially expressed genes (DEGs) comparing resistant to susceptible snails

The present RNAseq approach conducted on whole snails, allow us to identify differentially expressed genes between resistant and susceptible phenotypes (Figures S1 to S3). The output file from DEseq2, comprising 21 296 genes, was filtered to select relevant DEGs with p-adjusted values < 0.01, and log2FoldChange > 1 or <-1. Applying these cut-off values resulted in 328 differentially expressed genes (DEGs), of which 129 were over-expressed and 199 down-regulated in the resistant snails compared to susceptible snails (Figure 1, Figure S4 and Table S2).

The first analysis was focused on a gene-by-gene approach on DEG functions and a particular attention was paid to the 50 genes over or down-regulated with the higher Log2fold change ratio (Figure 2, Table S2, Figure S4). Interestingly a large number of genes belonging to multigenic families are both over- and down-regulated. These genes belong mainly to the ankyrin (3 genes up/3 genes down), GTP IMAP-AIG (2 genes up/2 genes down), C-type lectin (1 gene up/1 gene down) and E3 ubiquitin ligase-XIAP-like (1 gene up/4 genes down) families (Table S2).

3.1.1 Over expressed genes in resistant snails

For the top 50 over-expressed genes (Table S2), most of the genes identified were involved in functions that include cell–cell signaling, cytoskeleton integrity, transcription and cell–cycle regulation, cell development, and various transport phenomena. More precisely, genes were identified that are involved in protein-protein interaction (Kelch protein), cell development and immunity (CUB and sushi domain-containing protein), cell-cell binding (floculin), cell signaling (ankyrin), apoptosis regulation (E3 ubiquitin ligase-XIAP-like, apoptosis inhibitor), modulation of chromatin structure, transcription, replication, recombination, and DNA repair (Poly (ADP-ribose) polymerases (PARPs) and ADP-ribosyltransferase diphtheria toxin-like : ARTD enzymes). Finally, numerous enzymes and proteases were also differentially expressed in resistant snails compared to susceptible as for example, endoglucanase involved in the degradation of complex natural carbohydrate substrates; Group XVI phospholipase A2 a thiol hydrolase that regulates lipolysis (Zhou et al., 2019); Acidic mammalian chitinase and Endo-chitosanase C major digestive enzymes that constitutively degrades chitin; serine proteases

with vast functions such as protein metabolism, digestion, blood coagulation, apoptosis, immunity regulation or fertilization (Patel, 2017).

Finally, few gene functions appeared to be related to lipid metabolism with sphingolipid activator protein (SAPs or saposins) essential cofactors for the lysosomal degradation of membrane-anchored sphingolipids and the low-density lipoprotein receptor-related protein a protein forming a receptor found in cell plasma membrane involved in signal transduction and receptor-mediated endocytosis.

3.1.2 Under expressed genes in resistant snails

Concerning the top 50 down-regulated genes (Table S2), interestingly most of the functions were shared with over-expressed genes, except specific down regulated genes as for example, HSP70 heat shock proteins performing chaperoning functions for protein folding, and protect cells from the adverse effects of physiological stresses; Chitin synthase 1 and chitin synthase chs-2-like isoform X2 involved in chitin synthesis associated with periostracum and radula biosynthesis in gastropods; BTB/POZ domain-containing protein a versatile protein-protein interaction motif that participates in a wide range of cellular functions, including transcriptional regulation, cytoskeleton dynamics, ion channel assembly and gating, and targeting proteins for ubiquitination; cell death abnormality protein 1 involved in apoptosis; and finally genes that could be related to immune functions like Techylectin-5B a lectin with a FREd domain and the activated leukocyte cell adhesion molecule CD-antigen (CD166) that regulates cellular signaling and cell dynamic responses.

3.1.3 Immune related functions of differentially expressed genes

It is interesting to note that some of the genes already described can have dual roles and are known in addition to their more overall functions to be also involved in inflammatory and immune response. Other genes are known for their well described functions in innate immunity. This lead us to consider that 30% of the 50 most over-expressed genes and 22% of the down-regulated genes belong to immune functions or to the internal defense system of *B. glabrata* (Table S2). In particular, we can specify that the CUB and sushi domain-containing proteins over expressed in resistant snails are part of a regulatory network of proteins known as "regulators of complement activation (RCA)". A subset of this family of proteins, complement control proteins (CCP), are characterized by the "Sushi" domain that prevent activation of the complement system on the surface of host cells and protect host tissues against damage caused by autoimmunity (Escudero-Esparza et al., 2013). Ankyrins are known

to be involved in inflammatory response. AIG1-like protein or GTPases of immunity-associated protein (GIMAP) are a distinctive family of GTPases, which control apoptosis in lymphocytes and play a central role in lymphocyte maturation and lymphocyte-associated diseases in infection context, linked to self-defense and development of T cells in vertebrates (Schwefel et al., 2010). Interleukin 17d is part of a family of cytokines, which was identified relatively recently in vertebrates as involved in host defense by controlling T cell activity by suppressing the function of dendritic cells (Lee et al., 2019; Liu et al., 2020). Then we identify some genes as up or down regulated, that functioned as pattern recognition receptors (PRRs) of the innate immune response belonging to C-type lectin (calcium dependent lectins), Techylectin-5B (FREd domain lectins) and fucolectin ("F-type" fold lectin) a newly identified family of fucose binding lectins (Wang et al., 2018). Finally, antimicrobial peptides (AMPs) mytimacin or neuromacin have been also identified.

3.2 Ranked-Based Gene Ontology Analysis (RBGOA) enrichment: A Gene Ontology approach

To go further in the identification of biological functions differentially represented in resistant snails versus susceptible ones, we conducted a functional enrichment analysis using the RBGOA and STRING packages. A total of 124 Gene Ontology (GO) over-represented terms were identified from the 129 over-expressed genes, while 225 over-represented GO terms were derived from the 199 down-regulated genes in the "Biological Process" category (Table S3). A total of 65 over-represented "Molecular Functions" were identified for both the over-expressed and down-regulated genes (Table S4). Then, the identified GO terms were aggregated into broader representative categories to provide a more synthesized understanding of the functional landscape.

In the resistant phenotype within the over expressed genes, several "Biological Processes" were found to be over-represented. The most represented functions were associated with general cell processes and particularly cell signalling pathways, cell development and communication, cell death, and O-glycan processing. Less represented functions were also enriched including phospholipase D activity, positive regulation of protein mono-ubiquitination, entry of bacterium into host cell, t-RNA-end processing, cell-cell adhesion mediated by cadherin, and prostaglandin catabolic process as shown in the Treemap

representation of over-represented “Biological Process” from over-expressed genes obtained from Revigo software (Figure 3, Table S3).

We identified also several over-represented “Biological Process” for genes down-regulated in resistant snails (Figure 4, Table S3). The main represented functions were: cell communication, development and sensory system and amino sugar metabolic process. Other functions were also enriched but associated with fewer GO terms, as for example peptidyl-arginine methylation, methylation, protein refolding, folic acid biosynthesis process, ubiquitin-dependent endocytosis, positive regulation of mitochondrial calcium ion concentration, or response to sulfur dioxide (Figure 4, Table S3). It is interesting to note that within the category “cell development and communication” for over-represented functions or over-expressed genes, specific GO terms were related to immunity, such as “organ or tissue specific immune response” and “mucosal immune response” (Table S3). However, most of the genes identified as differentially expressed have dual or pleiotropic functions and this may explain why there aren't more immunity-related terms appearing in our overall analyses.

In the case of the over-represented “Molecular Function” category within the over-expressed genes from resistant phenotype, we observed several enriched functions including tumor necrosis factor receptor activity, apolipoprotein receptor activity, sphingolipid activator protein activity, fucosyltransferase activity, prostaglandin-reductase activity, FBXO family protein binding, and catalytic activity on a glycoprotein (Figure S4, Table S4). All these GO terms can be related to protein-protein interactions, signal transduction, cell activation, cell death pathways or apoptosis and lipid metabolism.

In examining the over-represented “Molecular Functions” of down-regulated genes for the resistant phenotype, we identified several activities including chitin synthase activity, hydrolase activity, adenosine receptor binding, protein-glycine ligase activity, linoleic acid epoxygenase activity, transcription regulator activator activity, ATP-dependent protein disaggregase activity, and osmolarity-sensing monoatomic cation channel activity (Figure S5, Table S4). All these activities belong mainly to various enzymatic processes involved in cell activity and metabolism.

3.3 STRING-DB analysis: KEGG pathway enrichment

Subsequently, we conducted a functional enrichment analysis based on KEGG (Kyoto Encyclopedia of Genes and Genomes) to elucidate the metabolic pathways that are mainly

associated with either over-expressed or down-regulated genes in the resistant phenotype. From the 328 differentially expressed genes, 57 genes were identified in metabolic pathways listed in the KEGG database. However, it is important to note that invertebrate models are generally not referenced in these databases, resulting in limited gene annotations. However, these 57 genes provide a valuable basis for further exploration of the molecular basis associated with resistant snail phenotype.

Results of the KEGG analysis revealed several pathways represented by the higher number of genes that are involved in folding, sorting and degradation that govern protein maturation and turnover, in addition to carbohydrate metabolism, transport and catabolism pathways (Figure 5). Interestingly, most of the pathways identified were supported by over-expressed and down-regulated genes indicating that the regulation of the pathway necessitates a balanced-gene expression, which requires potentially the repression of certain sub-pathways within the metabolic pathway considered to allow the expression of other sub-pathways. Thus, we decided to pay a particular attention to the pathways that are mainly represented by over-expressed genes (Figure 5). We do not consider the “immune system” pathway because it is represented by only 1 gene. The 2 other pathways to be considered were the “Lipid metabolism pathways” and “Signalling molecules and interaction pathway” (Figure 5 and Table S5). The convergence of these pathways highlights a biochemical framework essential to the resistant phenotype. Among the array of pathways identified, lipid metabolism distinctly stands out within the resistance phenotype. Remarkably, except sphingolipid metabolism that is associated with an down-regulated gene (BGLB011932) all the other lipid pathways belong to over-expressed genes (BGLB037124; BGLB028216; BGLB031390), suggesting a potential up-regulation and consequent activation of lipid-related metabolic processes (Table S5). Given this unique pattern of expression, and the pathway's exclusive association with the resistance phenotype, we have elected to narrow our focus to the lipid expression profiles by conducting a functional exploration of these results thanks through a targeted metabolomic approach centred on lipids.

3.4 Targeted lipidomic analyses

Five biological replicates out of 6 were used in the present lipidomic approach (R2, R3, R4, R5, R6 for resistant and S1, S2, S3, S4, S5 for susceptible snails ; Figure S6). To identify differentially expressed lipid metabolites between resistant and susceptible snails, a Bonferroni correction

was applied to all quantitiative metabolite data, and lipid metabolites with a p-adjusted < 0.05 were selected (Figure 6, Table S6).

The comprehensive lipidomic analysis was conducted on a total of 419 metabolites. Among these, 24 metabolites were identified as being significantly and differentially modulated between susceptible and resistant snail replicates (Table S6). In the lipid analysis of the resistant samples, we identified several lipid families as being over-represented. These include phosphatidylethanolamine, acylcarnitine, dihydroceramide, alkenylphosphatidylcholine (plasmalogen), and alkenylphosphatidylethanolamine (Figure 6, Table S6). The lipid families identified as under-represented in the resistant phenotype include ceramide, deoxyceramide, alkylphosphatidylethanolamine, sphingomyelin, lysoalkenylphosphatidylethanolamine (plasmalogen), fatty acid, ubiquinone, lysophosphatidylethanolamine, and methyl-cholesteryl ester (Figure 6, Table S6).

This analysis reveals a notable change in lipid composition in resistant snails with a decrease in represented sphingolipids, such as ceramide and sphingomyelin, in favour of glycerophospholipids such as phosphatidylethanolamine. The sphingolipids, phosphatidylethanolamine and phosphatidylcholine are major components of biological membranes and thus may hint at a differential membrane asymmetry between resistant and susceptible snails. Moreover, acylcarnitine enable fatty acids to cross mitochondrial membranes and be degraded by β-oxidation. The β-oxidation is the main metabolic pathway for energy production through the respiratory chain and oxidative phosphorylation to form ATP molecules. The observation that acylcarnitine is over-represented and fatty acid are under-represented in resistant snails could be an argument to hypothesize that energy production is greater in resistant than in susceptible snails. Even if ubiquinone that acts as electron carrier in the respiratory chain is under-represented in resistant snails. Thus, to verify this hypothesis we conducted an ATP titration in whole snails from resistant and susceptible phenotypes.

3.5 Adenosine Tri-Phosphate quantification in resistant and susceptible snails:

By comparing ATP levels between resistant and susceptible samples, we aimed to unveil any significant differences in energy metabolism that might contribute to the difference in phenotype observed. However, no significant difference was observed in ATP concentrations (Mann-Whitney U-test =12 ; pvalue = 0.06) (Table S7). Thus, the present analysis did not reveal

any discernible variations in energy metabolism between the resistant and susceptible snail samples.

4 Discussion

The question of snail/schistosome compatibility has particularly attracted the attention of the scientific community in the past 20 years and numerous studies have been conducted to elucidate the molecular basis of such interaction (Coustau et al., 2015; Li et al., 2020; Mitta et al., 2017; Portet et al., 2019). The developments of comparative genomics, transcriptomics, and proteomics or targeted approaches have enabled research groups to investigate the underlying molecular determinants using different laboratory strains or selected lines of snails and schistosomes. Genetic studies of crosses between snail consanguineous lines displaying compatible and incompatible phenotypes have revealed some candidate loci, including a gene cluster containing a super-oxide dismutase (SOD)-encoding gene (Allan et al., 2017; Blouin et al., 2013; Bonner et al., 2012; Goodall et al., 2006) and differential allelic expressions of the SOD gene in different individuals of the predominantly resistant 13-16-R1 strain of *B*. *glabrata* have been demonstrated (Abou-El-Naga et al., 2015; Goodall et al., 2006). RAD-seq and GWAS approaches developed on the *Biomphalaria glabrata* Guadeloupe strain or used to compared resistant strain BS90 and the susceptible strain M-line showed correlation between compatibility phenotype and multi-genic regions GRC (Guadeloupean resistance complex), PTC1 (Polymorphic transmembrane 1) (Tennessen et al., 2015b) or PTC2 (Tennessen et al., 2020) that contains 11 genes, 9 of which code for transmembrane proteins (Blouin et al., 2022). Gene functions in these clusters were not clearly defined, but they have been putatively associated with parasite recognition (Tennessen et al., 2015b). Various transcriptomic comparisons have also been performed on other compatible and incompatible strains of snails and schistosomes isolated from different geographic localities (Adema et al., 2010; Duval et al., 2020; Hanington et al., 2010; Ittiprasert et al., 2010; Pila et al., 2016; Pinaud et al., 2021; Portet et al., 2019, 2019).

In such studies, the main differentially expressed immune relevant transcripts were involved in immune cellular responses, cell adhesion, extra cellular matrix composition, cell migration, cell differentiation and cell proliferation and belong to (i) immune recognition molecules (fibrinogen-related proteins (FREPs) 2, 3, 4, 6 and 11, 12, CREPs, GREPS, C-type lectins, Toll-like

receptor, galectins, or PGRP, GNBP) (ii) immune signalling molecules (Thioester-containing proteins (TEP), alpha-2 macroglobulin receptor, cytokines, macrophage migration inhibitory factor (MIF), macrophage mannose receptor, dermatopontin, C1q-like lectins involved in the complement pathway, heat shock proteins (HSP)) or (iii) immune effectors (oxidative stress superoxide dismutases (Cu-Zn SOD, SOD chaperone and SOD Mn), dual oxidase, antimicrobial molecules (antimicrobial peptides (AMPs), lipopolysacharide (LPS) binding proteins, LBP-BPI, lysozyme) and biomphalysin). Moreover, the association of some of these molecules into protein complex dedicated to parasite killing have been demonstrated.

Indeed, association between humoral immune molecules; *Bg*FREP2, *Bg*FREP3, *Bg*TEP1, and Biomphalysin for targeting parasite antigens (Galinier et al., 2017; Li et al., 2020; Moné et al., 2010) seems to initiate haemocyte-mediated destruction of *S. mansoni* sporocysts and partly explains the resistance to *S. mansoni* in this model.

In the present study, our investigation unveiled molecules and functions bearing semblance to those previously identified. Indeed, we identified lectins (C-type lectin, fucolectin or CREPs) acting as immune recognition molecules. We also identified molecules involved in cellular adhesion, differentiation, or immune effectors like AMPs (Table S2). But intriguingly, we notice the absence of classically observed immune candidates like FREPs, TEPs (Duval et al., 2020) or Biomphalysins (Pinaud et al., 2021) in favour of molecules more related to more general cell functions or metabolism. Genes involved in protein-protein interaction, cell development / binding / signalling / apoptosis or DNA transcription / replication / recombination / repair were identified (Table S2). Finally, numerous enzymes and proteases were also differentially expressed and gene functions related to lipid / fatty acid metabolism were highly represented in resistant snails compared to susceptible.

To explain this inconsistency with anterior results it is important to consider that herein we analyse the molecular basis of *Schistosoma*/*Biomphalaria* compatibility. But rather than comparing totally different geographic isolates with different co-evolutive histories and genetic backgrounds or clonal selected lines of snails as done before, we conduct a molecular comparative analysis on snail strains with the same genetic background, without loss of genetic diversity due to cross breeding. We could hypothesis that this new selection approach may explain this discrepancy.

Notably we identify some differences on two pathways that were particularly over-represented in resistant snails which correspond to the “Lipid metabolism pathways” and the “Signalling molecules and interaction pathway” (Figure 5 and Table S5). Lipid metabolism distinctly stands out within sphingolipid metabolism that is associated with an down-regulated gene (BGLB011932) and other lipid pathways were associated with over-expressed genes (BGLB037124; BGLB028216; BGLB031390). Interestingly, those RNAseq results were confirmed by the lipidomic approach that demonstrated a notable change in lipid composition in resistant snails with a decrease in represented sphingolipids, such as ceramide, deoxyceramide and sphingomyelin, in favour of glycerophospholipids such as alkenyl-phosphatidylcholine, alkenyl-phosphatidylethanolamine and phosphatidylethanolamine. Moreover, the accumulation of dihydroceramide belonging to sphingolipid pathway (Figure 6), is a hallmark of the reduced ceramide production, as it acts as precursor of ceramide (Rahmaniyan et al., 2011). Phospholipids and sphingolipids are not simply passive constituents of cell plasma membranes but have important roles in numerous cellular functions like protein biogenesis and activity, energy production by oxidative phosphorylation, mitochondrial stability, autophagy, apoptosis, reactive oxygen species defence, cell behaviour (adherence, cell shape, motility, membrane fusion, vacuolation, phagocytosis) and cell signalling (membrane microdomains/lipid rafts) (Breslow and Weissman, 2010; Calzada et al., 2016; Tang et al., 2022).

Herein, the differential regulation of acylcarnitine, fatty acid and ubiquinone (Figure 6) involved in the mitochondrial respiratory chain led us to hypothesize a difference in energy metabolism between susceptible and resistant individuals. However, the ATP concentration is similar when comparing resistant and susceptible phenotypes (Table S7). Thus, the change in lipid content observed in the present study does not appear to be related to energy metabolism. As lipids play important roles in many biological functions, it is clear that other alternative hypotheses need to be considered.

Membrane lipid asymmetry is another important aspect of cell functions (van Meer, 1989), for the mechanical stability of the membrane (fluidity or stiffness), vesicular transport, cell cycle progression or apoptosis (Hissa et al., 2012). The major lipid components of the eukaryotic plasma membrane include glycerophospholipids, sphingolipids, and cholesterol that are irregularly distributed between the two leaflet: phosphatidylserine (PS) (not differentially regulated in resistant snails) and phosphatidylethanolamine (PE) (over represented in

resistant) are concentrated in the inner leaflet, whereas phosphatidylcholine (PC) (over represented in resistant) and sphingomyelin (SM) (under-represented in resistant) are concentrated in the outer leaflet. The cholesterol (CE), an essential structural component of animal cell membranes, known to regulate partly the membrane fluidity, is also significantly under-represented in resistant snails (Figure 6). The potential increase of PE in the inner leaflet, reduction of SM in favour of PC in the outer leaflet and reduction of CE within the two leaflets may hint for a modification of membrane asymmetry and structure between resistant and susceptible snails. Moreover, decrease of SM content and CE depletion have been also associated with a significant decrease in membrane stiffness (Horváth et al., 2022; Weber et al., 2010) . All these changes in membrane lipid content in resistant snails may lead to different cellular shape, adhesion, motility, resulting in an overall modification of their cellular behavior (Ramprasad et al., 2007). Understanding how this overall differences in membrane dynamic between resistant and susceptible snails affect their phenotypes will necessitate further researches for answering this intriguing question.

Another important aspect linked to membrane lipids is cell signalling. Sphingomyelin and cholesterol-enriched localized domains in the outer-leaflet form lipid microdomains known as lipid rafts (Simons and Ikonen, 1997) that play several roles in cell signalling, signal transduction and membrane trafficking (Hanzal-Bayer and Hancock, 2007; Ohanian and Ohanian, 2001). The low level of SM and CE in resistant snails would thus potentially results in a modification of signalling and signal transduction related to lipid rafts in resistant phenotypes potentially in favour of other cell signalling pathways. Thus we can hypothesis that cell signalling in resistant snails may therefore be different, but better adapted to respond effectively to the presence of the parasite.

By altering the lipid composition of their cell membrane, living organisms may adapt to environmental stress, this strategy of membrane adaptation is termed homeoviscous adaptation (Ernst et al., 2016; Herrera et al., 2021; Oger, 2015). In the present host-parasite context, we can hypothesis that changes in lipid composition of cell membrane for resistant snails may affect the function of biomolecules residing within or associated with the membrane, impacting membrane-dependent functions and cell signalling. Consequently, the molecular dialogue between the parasite and the host may be impaired resulting in an unsuitability between the host and the parasite. The parasite would be in the incapacity to immunomodulate or circumvent the host immune system whereas this physiological suitability

with the host is absolutely necessary for the successful development of parasite (Wiedenmann and Smith, 1997). It has been demonstrated that the parasite needs to exploit the host's lipids for its own development and growth (Gonçalves-Silva et al., 2022; von Bülow et al., 2023), this being pivotal for parasite survival and propagation within the host (Allan et al., 1987). Homeoviscous adaptation of resistant hosts may reduce or impair the ability of parasites to exploit the host and thus their ability to survive in resistant host environment, making resistant snails better adapted to respond effectively to the presence of the parasite.

The aim of this comprehensive lipidomic analysis was to provide a detailed profile of the lipid categories present in each of the phenotypes. By integrating the lipidomic data with our transcriptomic results, we sought to obtain a better understanding of lipid dynamics and their potential role in the acquisition of resistance. This multi-dimensional approach, which encompasses transcriptomic and lipidomic analyses, enables a more nuanced exploration of the molecular mechanisms underlying resistance and may offer new insights into the metabolic changes associated with the resistant phenotype.

The insights gained from identifying and understanding these key metabolic pathways may pave the way for uncovering potential metabolic targets for modulating resistance and may also provide a foundational framework for further mechanistic studies investigating the interplay between metabolic regulation and resistance. The RNAseq and metabolic data amassed herein presents a compelling database for elucidating the phenotypic dichotomy of resistance and susceptibility against *Schistosoma mansoni* in *Biomphalaria glabrata* and may uncover novel molecular pathways or mechanisms contributing to the observed phenotypes. These data may serve as valuable resources for the broader scientific community engaged in fighting schistosomiasis, thereby contributing to reveal new avenues for targeting resistance at the molecular level and delineating novel therapeutic targets.

Acknowledgment

The authors want to thank Damien Pouzol and Olivier Portela for their help in animal maintenance. Many thanks to Thierry Noguer, George Istamboulie, and Gaëlle Catanante from the B.A.E laboratory at the University of Perpignan Via Domitia for their help in luminometer reading.

Financial supports:

This study is set within the framework of the “Laboratoires d’Excellences (LABEX)” TULIP (ANR-10-LABX-41) and CeMEB (ANR-10-LABX-04-01). RG, BG and DD were supported by the RIVOC (Risques Infectieux et Vecteurs en Occitanie) project ResiMetaMol. ES benefited from doctoral fellowships from Occitanie region. The authors wish to acknowledge French Ministry of Higher Education and Research for funding the Platform for Translational Oncometabolomics through a CPER grant (IBDLR). The funders had no role in study design, data collection and analysis, decision to publish, or preparation of the manuscript.

References

Abou-El-Naga, I.F., Sadaka, H.A.E.-M., Amer, E.I., Diab, I.H., Khedr, S.I.A.E.-H., 2015. Impact of the age of Biomphalaria alexandrina snails on Schistosoma mansoni transmission: modulation of the genetic outcome and the internal defence system of the snail. Mem Inst Oswaldo Cruz 110, 585–595. https://doi.org/10.1590/0074-02760150016

Adema, C.M., Hanington, P.C., Lun, C.-M., Rosenberg, G.H., Aragon, A.D., Stout, B.A., Lennard Richard, M.L., Gross, P.S., Loker, E.S., 2010. Differential transcriptomic responses of Biomphalaria glabrata (Gastropoda, Mollusca) to bacteria and metazoan parasites, Schistosoma mansoni and Echinostoma paraensei (Digenea, Platyhelminthes). Molecular Immunology 47, 849–860. https://doi.org/10.1016/j.molimm.2009.10.019

Allan, D., Payares, G., Evans, W.H., 1987. The phospholipid and fatty acid composition of Schistosoma mansoni and of its purified tegumental membranes. Molecular and Biochemical Parasitology 23, 123–128. https://doi.org/10.1016/0166-6851(87)90147-2

Allan, E.R.O., Gourbal, B., Dores, C.B., Portet, A., Bayne, C.J., Blouin, M.S., 2018. Clearance of schistosome parasites by resistant genotypes at a single genomic region in Biomphalaria glabrata snails involves cellular components of the hemolymph. International Journal for Parasitology 48, 387–393. https://doi.org/10.1016/j.ijpara.2017.08.008

Allan, E.R.O., Tennessen, J.A., Bollmann, S.R., Hanington, P.C., Bayne, C.J., Blouin, M.S., 2017. Schistosome infectivity in the snail, Biomphalaria glabrata, is partially dependent on the expression of Grctm6, a Guadeloupe Resistance Complex protein. PLOS Neglected Tropical Diseases 11, e0005362. https://doi.org/10.1371/journal.pntd.0005362

Alonso, D., Muñoz, J., Gascón, J., Valls, M.E., Corachan, M., 2006. Failure of standard treatment with praziquantel in two returned travelers with Schistosoma haematobium infection. Am J Trop Med Hyg 74, 342–344.

Altschul, S.F., Gish, W., Miller, W., Myers, E.W., Lipman, D.J., 1990. Basic local alignment search tool. Journal of Molecular Biology 215, 403–410. https://doi.org/10.1016/S0022-2836(05)80360-2

Alwan, S.N., Taylor, A.B., Rhodes, J., Tidwell, M., McHardy, S.F., LoVerde, P.T., 2023. Oxamniquine derivatives overcome Praziquantel treatment limitations for Schistosomiasis. PLOS Pathogens 19, e1011018. https://doi.org/10.1371/journal.ppat.1011018

Basch, P.F., 1975. An interpretation of snail-trematode infection rates: specificitity based on concordance of compatible phenotypes. Int J Parasitol 5, 449–452. https://doi.org/10.1016/0020-7519(75)90012-0

Blouin, M.S., Bollmann, S.R., Tennessen, J.A., 2022. PTC2 region genotypes counteract Biomphalaria glabrata population differences between M-line and BS90 in resistance to infection by Schistosoma mansoni. PeerJ 10, e13971. https://doi.org/10.7717/peerj.13971

Blouin, M.S., Bonner, K.M., Cooper, B., Amarasinghe, V., O'Donnell, R.P., Bayne, C.J., 2013. Three genes involved in the oxidative burst are closely linked in the genome of the snail, Biomphalaria glabrata. International Journal for Parasitology 43, 51–55. https://doi.org/10.1016/j.ijpara.2012.10.020

Bonner, K.M., Bayne, C.J., Larson, M.K., Blouin, M.S., 2012. Effects of Cu/Zn Superoxide Dismutase (sod1) Genotype and Genetic Background on Growth, Reproduction and Defense in Biomphalaria glabrata. PLOS Neglected Tropical Diseases 6, e1701. https://doi.org/10.1371/journal.pntd.0001701

Breslow, D.K., Weissman, J.S., 2010. Membranes in balance: mechanisms of sphingolipid homeostasis. Mol Cell 40, 267–279. https://doi.org/10.1016/j.molcel.2010.10.005

Calzada, E., Onguka, O., Claypool, S.M., 2016. Chapter Two - Phosphatidylethanolamine Metabolism in Health and Disease, in: Jeon, K.W. (Ed.), International Review of Cell and Molecular Biology. Academic Press, pp. 29–88. https://doi.org/10.1016/bs.ircmb.2015.10.001

Chida, J., Yamane, K., Takei, T., Kido, H., 2012. An efficient extraction method for quantitation of adenosine triphosphate in mammalian tissues and cells. Analytica Chimica Acta 727, 8–12. https://doi.org/10.1016/j.aca.2012.03.022

Chong, J., Wishart, D.S., Xia, J., 2019. Using MetaboAnalyst 4.0 for Comprehensive and Integrative Metabolomics Data Analysis. Curr Protoc Bioinformatics 68, e86. https://doi.org/10.1002/cpbi.86

Coustau, C., Gourbal, B., Duval, D., Yoshino, T.P., Adema, C.M., Mitta, G., 2015. Advances in gastropod immunity from the study of the interaction between the snail Biomphalaria glabrata and its parasites: A review of research progress over the last decade. Fish & Shellfish Immunology 46, 5–16. https://doi.org/10.1016/j.fsi.2015.01.036

Couto, F.F.B., Coelho, P.M.Z., Araújo, N., Kusel, J.R., Katz, N., Jannotti-Passos, L.K., Mattos, A.C.A., 2011. Schistosoma mansoni: a method for inducing resistance to praziquantel using infected Biomphalaria glabrata snails. Mem Inst Oswaldo Cruz 106, 153–157. https://doi.org/10.1590/s0074-02762011000200006

Dobin, A., Davis, C.A., Schlesinger, F., Drenkow, J., Zaleski, C., Jha, S., Batut, P., Chaisson, M., Gingeras, T.R., 2013. STAR: ultrafast universal RNA-seq aligner. Bioinformatics 29, 15–21. https://doi.org/10.1093/bioinformatics/bts635

Duval, D., Pichon, R., Lassalle, D., Laffitte, M., Gourbal, B., Galinier, R., 2020. A New Assessment of Thioester-Containing Proteins Diversity of the Freshwater Snail Biomphalaria glabrata. Genes (Basel) 11. https://doi.org/10.3390/genes11010069

Ernst, R., Ejsing, C.S., Antonny, B., 2016. Homeoviscous Adaptation and the Regulation of Membrane Lipids. J Mol Biol 428, 4776–4791. https://doi.org/10.1016/j.jmb.2016.08.013

Escudero-Esparza, A., Kalchishkova, N., Kurbasic, E., Jiang, W.G., Blom, A.M., 2013. The novel complement inhibitor human CUB and Sushi multiple domains 1 (CSMD1) protein promotes factor I-mediated degradation of C4b and C3b and inhibits the membrane attack complex assembly. FASEB J 27, 5083–5093. https://doi.org/10.1096/fj.13-230706

Fallon, P.G., Doenhoff, M.J., 1994. Drug-resistant schistosomiasis: resistance to praziquantel and oxamniquine induced in Schistosoma mansoni in mice is drug specific. Am J Trop Med Hyg 51, 83–88. https://doi.org/10.4269/ajtmh.1994.51.83

Famakinde, D.O., 2018. Treading the Path towards Genetic Control of Snail Resistance to Schistosome Infection. Trop Med Infect Dis 3, 86. https://doi.org/10.3390/tropicalmed3030086

Galinier, R., Roger, E., Moné, Y., Duval, D., Portet, A., Pinaud, S., Chaparro, C., Grunau, C., Genthon, C., Dubois, E., Rognon, A., Arancibia, N., Dejean, B., Théron, A., Gourbal, B., Mitta, G., 2017. A multistrain approach to studying the mechanisms underlying compatibility in the interaction between Biomphalaria glabrata and Schistosoma mansoni. PLOS Neglected Tropical Diseases 11, e0005398. https://doi.org/10.1371/journal.pntd.0005398

Gonçalves-Silva, G., Vieira, L.G.M. dos S., Cosenza-Contreras, M., Souza, A.F.P., Costa, D.C., Castro-Borges, W., 2022. Profiling the serum proteome during Schistosoma mansoni infection in the BALB/c mice: A focus on the altered lipid metabolism as a key modulator of host-parasite interactions. Frontiers in Immunology 13.

Goodall, C.P., Bender, R.C., Brooks, J.K., Bayne, C.J., 2006. Biomphalaria glabrata cytosolic copper/zinc superoxide dismutase (SOD1) gene: association of SOD1 alleles with resistance/susceptibility to Schistosoma mansoni. Mol Biochem Parasitol 147, 207–210. https://doi.org/10.1016/j.molbiopara.2006.02.009

Götz, S., García-Gómez, J.M., Terol, J., Williams, T.D., Nagaraj, S.H., Nueda, M.J., Robles, M., Talón, M., Dopazo, J., Conesa, A., 2008. High-throughput functional annotation and data mining with the Blast2GO suite. Nucleic Acids Res 36, 3420–3435. https://doi.org/10.1093/nar/gkn176

Gryseels, B., Stelma, F.F., Talla, I., van Dam, G.J., Polman, K., Sow, S., Diaw, M., Sturrock, R.F., Doehring-Schwerdtfeger, E., Kardorff, R., 1994. Epidemiology, immunology and chemotherapy of Schistosoma mansoni infections in a recently exposed community in Senegal. Trop Geogr Med 46, 209–219.

Hanington, P.C., Lun, C.-M., Adema, C.M., Loker, E.S., 2010. Time series analysis of the transcriptional responses of Biomphalaria glabrata throughout the course of intramolluscan development of Schistosoma mansoni and Echinostoma paraensei. International Journal for Parasitology 40, 819–831. https://doi.org/10.1016/j.ijpara.2009.12.005

Hanzal-Bayer, M.F., Hancock, J.F., 2007. Lipid rafts and membrane traffic. FEBS Lett 581, 2098–2104. https://doi.org/10.1016/j.febslet.2007.03.019

Herrera, C.M., Voss, B.J., Trent, M.S., 2021. Homeoviscous Adaptation of the Acinetobacter baumannii Outer Membrane: Alteration of Lipooligosaccharide Structure during Cold Stress. mBio 12, 10.1128/mbio.01295-21. https://doi.org/10.1128/mbio.01295-21

Hissa, B., Duarte, J.G., Kelles, L.F., Santos, F.P., del Puerto, H.L., Gazzinelli-Guimarães, P.H., de Paula, A.M., Agero, U., Mesquita, O.N., Guatimosim, C., Chiari, E., Andrade, L.O., 2012. Membrane Cholesterol Regulates Lysosome-Plasma Membrane Fusion Events and Modulates Trypanosoma cruzi Invasion of Host Cells. PLoS Negl Trop Dis 6, e1583. https://doi.org/10.1371/journal.pntd.0001583

Horváth, Á., Erostyák, J., Szőke, É., 2022. Effect of Lipid Raft Disruptors on Cell Membrane Fluidity Studied by Fluorescence Spectroscopy. International Journal of Molecular Sciences 23, 13729. https://doi.org/10.3390/ijms232213729

Huerta-Cepas, J., Szklarczyk, D., Heller, D., Hernández-Plaza, A., Forslund, S.K., Cook, H., Mende, D.R., Letunic, I., Rattei, T., Jensen, L.J., von Mering, C., Bork, P., 2019. eggNOG 5.0: a hierarchical, functionally and phylogenetically annotated orthology resource based on 5090 organisms and 2502 viruses. Nucleic Acids Res 47, D309–D314. https://doi.org/10.1093/nar/gky1085

Huynh, K., Barlow, C.K., Jayawardana, K.S., Weir, J.M., Mellett, N.A., Cinel, M., Magliano, D.J., Shaw, J.E., Drew, B.G., Meikle, P.J., 2019. High-Throughput Plasma Lipidomics: Detailed Mapping of the Associations with Cardiometabolic Risk Factors. Cell Chem Biol 26, 71-84.e4. https://doi.org/10.1016/j.chembiol.2018.10.008

Ittiprasert, W., Miller, A., Myers, J., Nene, V., El-Sayed, N.M., Knight, M., 2010. Identification of immediate response genes dominantly expressed in juvenile resistant and susceptible Biomphalaria glabrata snails upon exposure to Schistosoma mansoni. Mol Biochem Parasitol 169, 27–39. https://doi.org/10.1016/j.molbiopara.2009.09.009

Jones, P., Binns, D., Chang, H.-Y., Fraser, M., Li, W., McAnulla, C., McWilliam, H., Maslen, J., Mitchell, A., Nuka, G., Pesseat, S., Quinn, A.F., Sangrador-Vegas, A., Scheremetjew, M., Yong, S.-Y., Lopez, R., Hunter, S., 2014. InterProScan 5: genome-scale protein function classification. Bioinformatics 30, 1236–1240. https://doi.org/10.1093/bioinformatics/btu031

Lee, Y., Clinton, J., Yao, C., Chang, S.H., 2019. Interleukin-17D Promotes Pathogenicity During Infection by Suppressing CD8 T Cell Activity. Front Immunol 10, 1172. https://doi.org/10.3389/fimmu.2019.01172

Li, H., Hambrook, J.R., Pila, E.A., Gharamah, A.A., Fang, J., Wu, X., Hanington, P., 2020. Coordination of humoral immune factors dictates compatibility between Schistosoma mansoni and Biomphalaria glabrata. eLife 9, e51708. https://doi.org/10.7554/eLife.51708

Liu, X., Sun, S., Liu, D., 2020. IL-17D: A Less Studied Cytokine of IL-17 Family. Int Arch Allergy Immunol 181, 618–623. https://doi.org/10.1159/000508255

Love, M.I., Huber, W., Anders, S., 2014. Moderated estimation of fold change and dispersion for RNA-seq data with DESeq2. Genome Biol 15, 550. https://doi.org/10.1186/s13059-014-0550-8

Mitta, G., Gourbal, B., Grunau, C., Knight, M., Bridger, J.M., Théron, A., 2017. Chapter Three - The Compatibility Between Biomphalaria glabrata Snails and Schistosoma mansoni: An Increasingly Complex Puzzle, in: Rollinson, D., Stothard, J.R. (Eds.), Advances in Parasitology. Academic Press, pp. 111–145. https://doi.org/10.1016/bs.apar.2016.08.006

Moné, Y., Gourbal, B., Duval, D., Pasquier, L.D., Kieffer-Jaquinod, S., Mitta, G., 2010. A Large Repertoire of Parasite Epitopes Matched by a Large Repertoire of Host Immune Receptors in an Invertebrate Host/Parasite Model. PLOS Neglected Tropical Diseases 4, e813. https://doi.org/10.1371/journal.pntd.0000813

Mulvey, M., Woodruff, D.S., 1985. Genetics of Biomphalaria glabrata: Linkage analysis of genes for pigmentation, enzymes, and resistance to Schistosoma mansoni. Biochem Genet 23, 877–889. https://doi.org/10.1007/BF00499935

Oger, P.M., 2015. Homeoviscous Adaptation of Membranes in Archaea. Subcell Biochem 72, 383–403. https://doi.org/10.1007/978-94-017-9918-8_19

Ohanian, J., Ohanian, V., 2001. Sphingolipids in mammalian cell signalling. CMLS, Cell. Mol. Life Sci. 58, 2053–2068. https://doi.org/10.1007/PL00000836

Patel, S., 2017. A critical review on serine protease: Key immune manipulator and pathology mediator. Allergologia et Immunopathologia 45, 579–591. https://doi.org/10.1016/j.aller.2016.10.011

Pila, E.A., Tarrabain, M., Kabore, A.L., Hanington, P.C., 2016. A Novel Toll-Like Receptor (TLR) Influences Compatibility between the Gastropod Biomphalaria glabrata, and the Digenean Trematode Schistosoma mansoni. PLoS Pathog 12, e1005513. https://doi.org/10.1371/journal.ppat.1005513

Pinaud, S., Tetreau, G., Poteaux, P., Galinier, R., Chaparro, C., Lassalle, D., Portet, A., Simphor, E., Gourbal, B., Duval, D., 2021. New Insights Into Biomphalysin Gene Family Diversification in the Vector Snail Biomphalaria glabrata. Front Immunol 12, 635131. https://doi.org/10.3389/fimmu.2021.635131

Portet, A., Pinaud, S., Chaparro, C., Galinier, R., Dheilly, N.M., Portela, J., Charriere, G.M., Allienne, J.-F., Duval, D., Gourbal, B., 2019. Sympatric versus allopatric evolutionary contexts shape differential immune response in Biomphalaria / Schistosoma interaction. PLoS Pathog 15, e1007647. https://doi.org/10.1371/journal.ppat.1007647

Rahmaniyan, M., Curley, R.W., Obeid, L.M., Hannun, Y.A., Kraveka, J.M., 2011. Identification of dihydroceramide desaturase as a direct in vitro target for fenretinide. J Biol Chem 286, 24754–24764. https://doi.org/10.1074/jbc.M111.250779

Ramprasad, O.G., Srinivas, G., Rao, K.S., Joshi, P., Thiery, J.P., Dufour, S., Pande, G., 2007. Changes in cholesterol levels in the plasma membrane modulate cell signaling and regulate cell adhesion and migration on fibronectin. Cell Motil Cytoskeleton 64, 199–216. https://doi.org/10.1002/cm.20176

Roger, E., Mitta, G., Moné, Y., Bouchut, A., Rognon, A., Grunau, C., Boissier, J., Théron, A., Gourbal, B.E.F., 2008. Molecular determinants of compatibility polymorphism in the Biomphalaria glabrata/Schistosoma mansoni model: new candidates identified by a global comparative proteomics approach. Mol Biochem Parasitol 157, 205–216. https://doi.org/10.1016/j.molbiopara.2007.11.003

Schwefel, D., Fröhlich, C., Eichhorst, J., Wiesner, B., Behlke, J., Aravind, L., Daumke, O., 2010. Structural basis of oligomerization in septin-like GTPase of immunity-associated protein 2 (GIMAP2). Proceedings of the National Academy of Sciences 107, 20299–20304. https://doi.org/10.1073/pnas.1010322107

Simons, K., Ikonen, E., 1997. Functional rafts in cell membranes. Nature 387, 569–572. https://doi.org/10.1038/42408

Szklarczyk, D., Kirsch, R., Koutrouli, M., Nastou, K., Mehryary, F., Hachilif, R., Gable, A.L., Fang, T., Doncheva, N.T., Pyysalo, S., Bork, P., Jensen, L.J., von Mering, C., 2023. The STRING database in 2023: protein–protein association networks and functional enrichment analyses for any sequenced genome of interest. Nucleic Acids Research 51, D638–D646. https://doi.org/10.1093/nar/gkac1000

Tang, H., Huang, X., Pang, S., 2022. Regulation of the lysosome by sphingolipids: Potential role in aging. J Biol Chem 298, 102118. https://doi.org/10.1016/j.jbc.2022.102118

Tennessen, J.A., Bollmann, S.R., Peremyslova, E., Kronmiller, B.A., Sergi, C., Hamali, B., Blouin, M.S., 2020. Clusters of polymorphic transmembrane genes control resistance to schistosomes in snail vectors. eLife 9, e59395. https://doi.org/10.7554/eLife.59395

Tennessen, J.A., Bonner, K.M., Bollmann, S.R., Johnstun, J.A., Yeh, J.-Y., Marine, M., Tavalire, H.F., Bayne, C.J., Blouin, M.S., 2015a. Genome-Wide Scan and Test of Candidate Genes in the Snail Biomphalaria glabrata Reveal New Locus Influencing Resistance to Schistosoma mansoni. PLOS Neglected Tropical Diseases 9, e0004077. https://doi.org/10.1371/journal.pntd.0004077

Tennessen, J.A., Théron, A., Marine, M., Yeh, J.-Y., Rognon, A., Blouin, M.S., 2015b. Hyperdiverse gene cluster in snail host conveys resistance to human schistosome parasites. PLoS Genet 11, e1005067. https://doi.org/10.1371/journal.pgen.1005067

Theron, A., Combes, C., 1995. Asynchrony of Infection Timing, Habitat Preference, and Sympatric Speciation of Schistosome Parasites. Evolution 49, 372–375. https://doi.org/10.2307/2410347

Theron, A., Rognon, A., Gourbal, B., Mitta, G., 2014. Multi-parasite host susceptibility and multi-host parasite infectivity: A new approach of the Biomphalaria glabrata/Schistosoma mansoni compatibility polymorphism. Infection, Genetics and Evolution 26, 80–88. https://doi.org/10.1016/j.meegid.2014.04.025

van Meer, G., 1989. Lipid traffic in animal cells. Annu Rev Cell Biol 5, 247–275. https://doi.org/10.1146/annurev.cb.05.110189.001335

Vera Alvarez, R., Pongor, L.S., Mariño-Ramírez, L., Landsman, D., 2019. TPMCalculator: one-step software to quantify mRNA abundance of genomic features. Bioinformatics 35, 1960–1962. https://doi.org/10.1093/bioinformatics/bty896

von Bülow, V., Gindner, S., Baier, A., Hehr, L., Buss, N., Russ, L., Wrobel, S., Wirth, V., Tabatabai, K., Quack, T., Haeberlein, S., Kadesch, P., Gerbig, S., Wiedemann, K.R., Spengler, B., Mehl, A., Morlock, G., Schramm, G., Pons-Kühnemann, J., Falcone, F.H., Wilson, R.A., Bankov, K., Wild, P., Grevelding, C.G., Roeb, E., Roderfeld, M., 2023. Metabolic reprogramming of hepatocytes by Schistosoma mansoni eggs. JHEP Rep 5, 100625. https://doi.org/10.1016/j.jhepr.2022.100625

Wang, Y., Xue, Z., Yi, Q., Wang, H., Wang, L., Lu, G., Liu, Y., Qu, C., Li, Y., Song, L., 2018. A novel fucolectin from Apostichopus japonicus with broad PAMP recognition pattern. Fish & Shellfish Immunology 77, 402–409. https://doi.org/10.1016/j.fsi.2018.04.013

Weber, P., Wagner, M., Schneckenburger, H., 2010. Fluorescence imaging of membrane dynamics in living cells. J Biomed Opt 15, 046017. https://doi.org/10.1117/1.3470446

Wiedenmann, R.N., Smith, J.W., 1997. Novel associations and importation biological control: the need for ecological and physiological equivalencies. Insect Science and its Application 17, 51–60.

William, S., Day, T.A., Botros, S., Tao, L.F., Bennett, J.L., Farghally, A., Ismail, M., Metwally, A., 1999. Resistance to praziquantel: direct evidence from Schistosoma mansoni isolated from Egyptian villagers. The American Journal of Tropical Medicine and Hygiene 60, 932–935. https://doi.org/10.4269/ajtmh.1999.60.932

Wright, R.M., Aglyamova, G.V., Meyer, E., Matz, M.V., 2015. Gene expression associated with white syndromes in a reef building coral, Acropora hyacinthus. BMC Genomics 16, 371. https://doi.org/10.1186/s12864-015-1540-2

Zhao, Y., Li, M.-C., Konaté, M.M., Chen, L., Das, B., Karlovich, C., Williams, P.M., Evrard, Y.A., Doroshow, J.H., McShane, L.M., 2021. TPM, FPKM, or Normalized Counts? A Comparative Study of Quantification Measures for the Analysis of RNA-seq Data from the NCI Patient-Derived Models Repository. Journal of Translational Medicine 19, 269. https://doi.org/10.1186/s12967-021-02936-w

Zhou, J., Mock, E.D., Martella, A., Kantae, V., Di, X., Burggraaff, L., Baggelaar, M.P., Al-Ayed, K., Bakker, A., Florea, B.I., Grimm, S.H., den Dulk, H., Li, C.T., Mulder, L., Overkleeft, H.S., Hankemeier, T., van Westen, G.J.P., van der Stelt, M., 2019. Activity-Based Protein Profiling Identifies α-Ketoamides as Inhibitors for Phospholipase A2 Group XVI. ACS Chem. Biol. 14, 164–169. https://doi.org/10.1021/acschembio.8b00969

Legends to figures

Figure 1: Volcano plot analysis of 328 selected differentially expressed genes (DEGs)

This volcano plot represents the differential expression analysis of 328 selected DEGs between resistant and susceptible phenotypes. Each point represents a gene, with the log2 fold change on the x-axis indicating the magnitude of differential expression and the -log10 p-value on the y-axis representing statistical significance. Genes with a corrected p-value of less than 0.01 are highlighted, distinguishing over-expressed genes (positive log2 fold change) from under-expressed genes (negative log2 fold change). The plot visually segregates genes significantly upregulated (in red on the right side) and downregulated (in blue on the left side) in the resistant phenotype compared to the susceptible phenotype.

Figure 2: TPM heatmap of the top 50 over-expressed and under-expressed genes among DEGs

This heatmap visualizes the expression levels of the top 50 over-expressed and top 50 under-expressed genes among the differentially expressed genes (DEGs) in resistant and susceptible snails. The expression levels are measured in TPM (Transcripts Per Million). Over-expressed genes are marked in red, while under-expressed genes are shown in blue. Each column represents one of the four biological replicates for either the resistant or susceptible phenotype. The Gene_Id labels correspond to genes identified from the *Biomphalaria glabrata* genome (BB02 version 1.7) available on VectorBase website. This figure provides a clear comparative view of gene expression patterns between the two phenotypes.

Figure 3: Treemap of GO terms for over-represented in over-expressed genes from biological process category

This treemap depicts the Gene Ontology (GO) terms for the biological process category, specifically for genes over-expressed in the resistance phenotype. The visualization is based on data processed through REVIGO. Each GO term, represented by rectangles, has a p-value of less than 0.01, indicating significant over-representation. The GO terms are grouped and color-coded according to larger biological process categories to enhance clarity and understanding of the data. This treemap provides an intuitive overview of the predominant biological processes associated with genes over-expressed in the resistance phenotype. See table S3 for details of the names in each square.

Figure 4: Treemap of gene ontology (GO) terms for over-represented in under-expressed genes from biological process category

This treemap visualizes Gene Ontology (GO) terms within the biological process category, corresponding to genes that are under-expressed in the resistance phenotype. This visual representation, derived from REVIGO, highlights GO terms that have a p-value of less than

0.01, signifying significant over-representation. The treemap organizes these terms into major groups, each distinguished by different colors representing various biological processes. This categorization and color-coding enhance the readability and interpretation of the data, allowing for an immediate grasp of the predominant biological processes associated with the under-expressed genes in the resistance phenotype. See table S3 for details of the names in each square.

Figure 5: Distribution of over and under-expressed genes across KEGG pathways

This bar chart provides a distribution analysis of unique genes across various KEGG (Kyoto Encyclopedia of Genes and Genomes) pathways, differentiating genes based on their expression status in the comparison of resistant (R) versus susceptible (S) phenotypes. Each bar represents a distinct KEGG pathway, with the height indicating the number of unique genes associated with that pathway. Over-expressed genes are indicated in red, while under-expressed genes are shown in blue. This visualization offers a clear depiction of the differential engagement of genes in specific pathways, highlighting the pathways that are most prominently affected in the resistant phenotype compared to the susceptible one.

Figure 6: Bar-plot of statistically significant lipid families based on log2FoldChange

This bar plot represents the sum log2 fold change in the abundance of various lipid families, derived from a targeted lipidomic analysis. Each bar corresponds to a different family of lipids, with the length of the bar indicating the magnitude of change (log2 fold change) in their abundance. Only those lipid families showing statistically significant changes are included. This graph provides a succinct overview of the lipidomic alterations, highlighting the families of lipids that are most significantly affected, thereby offering insights into the lipid metabolic changes associated with the studied conditions.

Supplementary files:

Figure S1: Principal Component Analysis (PCA) of RNAseq data from resistant and susceptible whole snail samples

This figure illustrates a Principal Component Analysis (PCA) performed on RNAseq data obtained from whole snail samples, categorized as resistant and susceptible. The PCA plot displays the distribution of samples along the two principal components: PC1 (Principal Component 1), which accounts for 53% of the variance, and PC2 (Principal Component 2), accounting for 15% of the variance. Samples from the susceptible condition are marked in red, while those from the resistant condition are in blue. The replicates are labelled as R1, R2, R3, R4 for resistant and S1, S2, S3, S4 for susceptible. This PCA plot provides a visual representation

of the overall variation in the transcriptomic data and the clustering patterns of the samples based on their phenotypic resistance or susceptibility.

Figure S2: Distance matrix and hierarchical clustering of resistant vs. susceptible

This figure presents a hierarchical clustering analysis based on a distance matrix derived from RNAseq data, comparing resistant and susceptible phenotypes. The distance matrix quantifies the dissimilarities between each pair of samples, reflecting the degree of difference in their gene expression profiles. The hierarchical clustering, depicted as a dendrogram, illustrates the relationships and relative distances between all samples, visually segregating them into clusters that correspond to the resistant and susceptible phenotypes.

Figure S3: Heatmap of 328 Differentially Expressed Genes (DEGs) in resistant vs. susceptible snails

Displayed in this heatmap is the expression profiling of 328 differentially expressed genes (DEGs) between resistant and susceptible snail phenotypes. Expression levels, measured in TPM (Transcripts Per Million), are visually represented for each gene across four replicates for both resistant and susceptible groups. Over-expressed genes are indicated in red, while under-expressed genes are shown in blue.

Figure S4: Treemap of Gene Ontology (GO) terms over-represented in over-expressed genes from molecular function category

This treemap illustrates the Gene Ontology (GO) terms in the molecular function category associated with genes that are over-represented in over-expressed genes in the resistance phenotype. The visualization, derived from REVIGO, highlights GO terms with a p-value of less than 0.01, indicating significant over-represented in this category. The GO terms are organized into major functional groups, each distinguished by a unique color to enhance the clarity of the displayed information. This graphical representation provides an intuitive understanding of the predominant molecular functions carried out by the over-expressed genes in the resistance phenotype, underscoring the specific functional roles these genes play. See table S4 for details of the names in each square.

Figure S5: Treemap of gene ontology (GO) terms over-represented in under-expressed genes from molecular function category

This figure showcases a treemap of Gene Ontology (GO) terms within the molecular function category, specifically for genes that are over-represented in under-expressed gene in the resistance phenotype. Created using REVIGO visualization, the treemap features GO terms that are significantly over-represented, as indicated by a p-value of less than 0.01. The terms are organized into large groups, differentiated by various colors corresponding to distinct

molecular functions. This color-coding and grouping strategy aids in clearly presenting the molecular functions predominantly associated with the under-expressed genes, thereby offering insights into the molecular mechanisms potentially involved in the resistance phenotype. See table S4 for details of the names in each square.

Figure S6: PLS-DA (Partial Least Squares-Discriminant Analysis) score plot for lipidomic analysis

This score plot represents the results of a Partial Least Squares-Discriminant Analysis (PLS-DA) applied to lipidomic data from resistant and susceptible snail samples. The x-axis depicts Component 1, which accounts for 23.6% of the variance, while the y-axis represents Component 2, accounting for 11.1% of the variance. In the plot, resistant replicates are denoted by red triangles, and susceptible replicates by green cross. The red and green circles indicate the respective clustering of the resistant and susceptible replicates. This visual representation provides a clear separation between the lipidomic profiles of resistant and susceptible phenotypes.

Figure 1

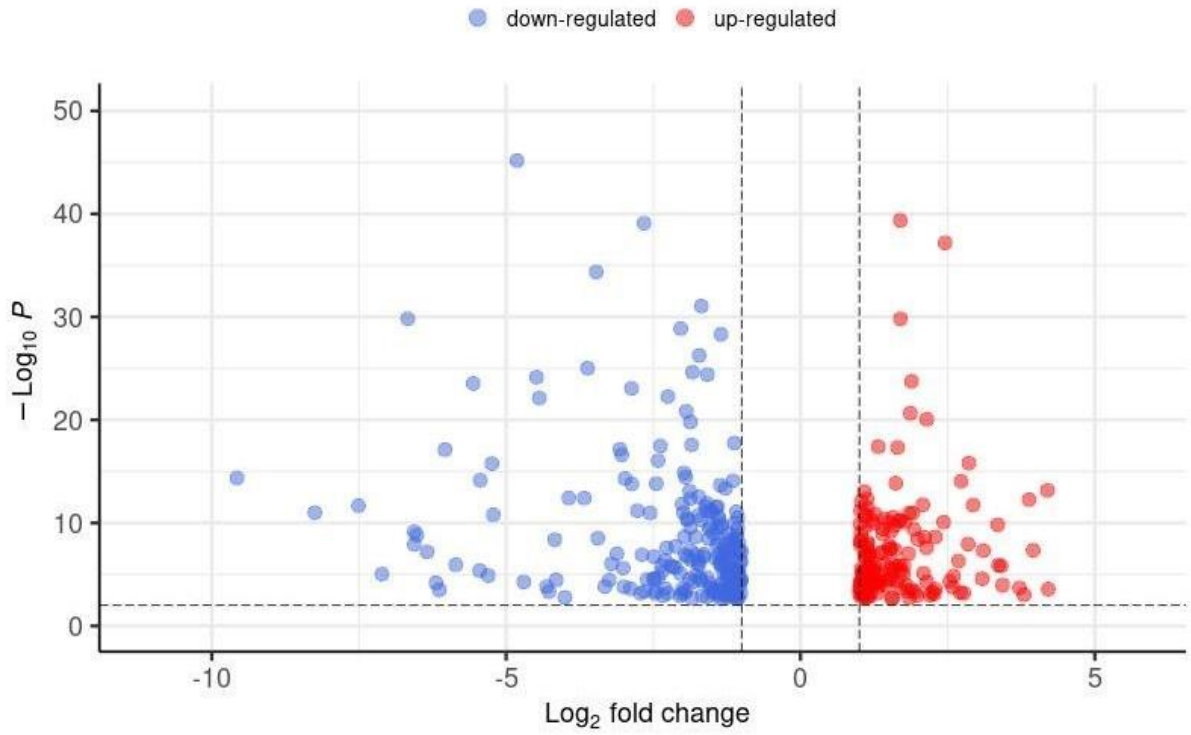
down-regulated
up-regulated
50
40
30
20
10
0
$-\text{Log}_{10}\ P$
-10
-5
0
5
Log_2 fold change

Figure 2

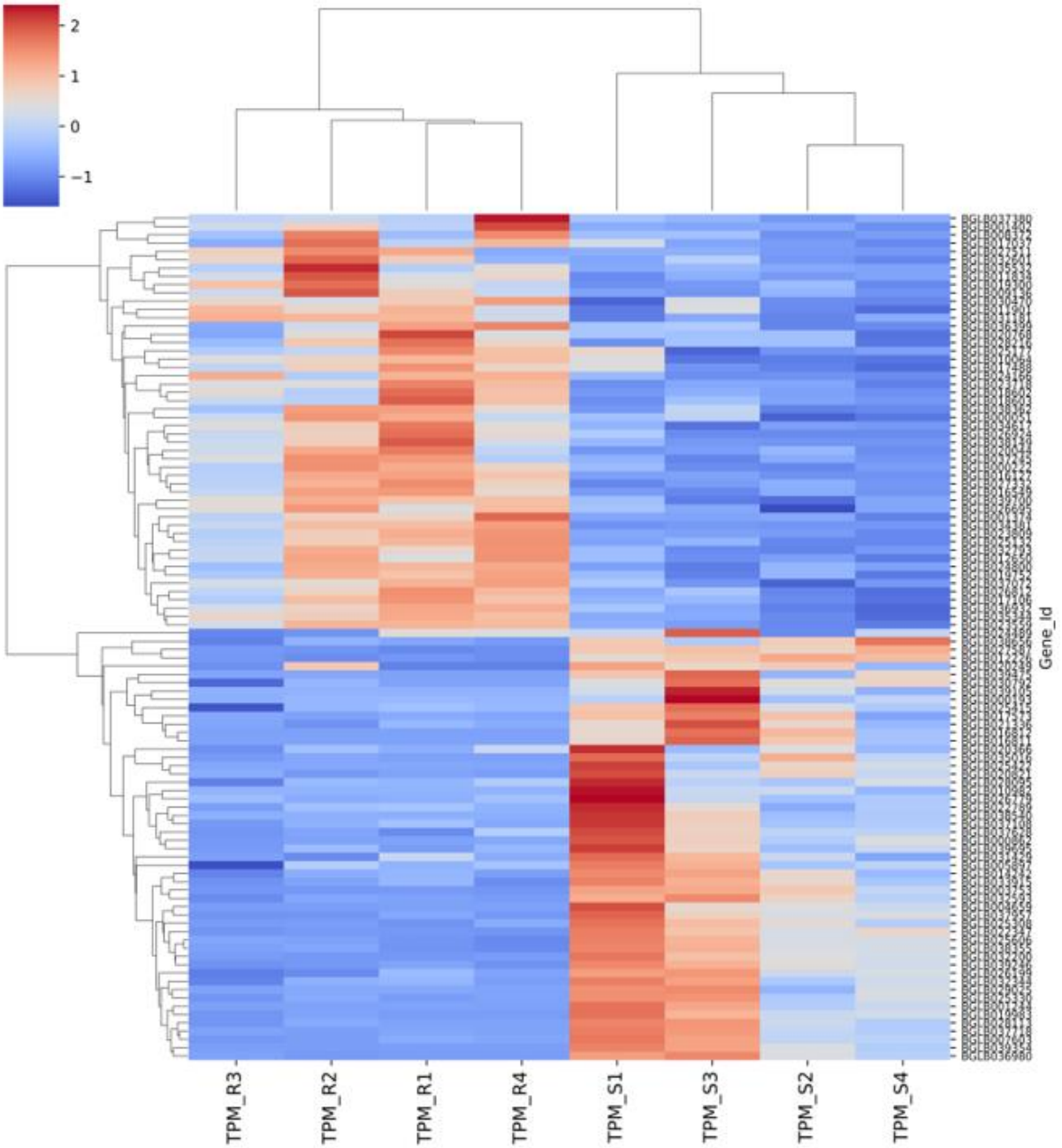
2
1
0
−1
TPM_R3
TPM_R2
TPM_R1
TPM_R4
TPM_S1
TPM_S3
TPM_S2
TPM_S4
Gene_Id

Figure 3

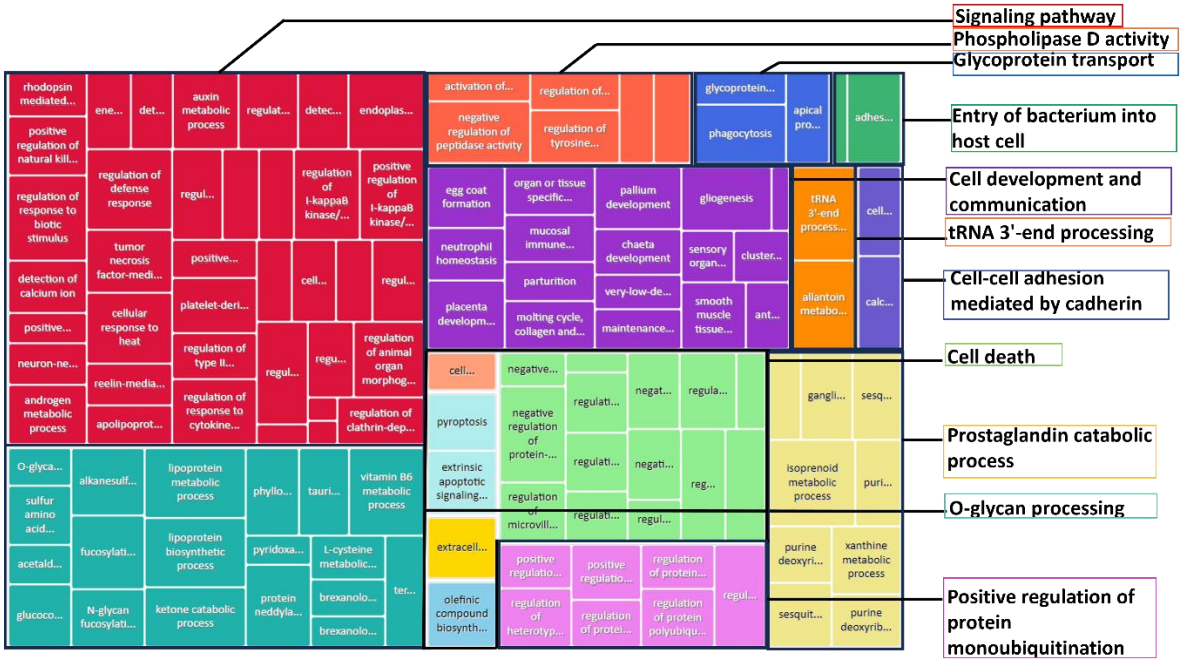
Signaling pathway
Phospholipase D activity
Glycoprotein transport
Entry of bacterium into host cell
Cell development and communication
tRNA 3'-end processing
Cell-cell adhesion mediated by cadherin
Cell death
Prostaglandin catabolic process
O-glycan processing
Positive regulation of protein monoubiquitination
rhodopsin mediated...
positive regulation of natural kill...
regulation of response to biotic stimulus
detection of calcium ion
positive...
neuron-ne...
androgen metabolic process
ene...
det...
auxin metabolic process
regulat...
detec...
endoplas...
regulation of defense response
regul...
regulation of I-kappaB kinase/...
positive regulation of I-kappaB kinase/...
tumor necrosis factor-medi...
positive...
cell...
regul...
cellular response to heat
platelet-deri...
reelin-media...
regulation of type II...
regul...
regu...
regulation of animal organ morphog...
apolipoprot...
regulation of response to cytokine...
regulation of clathrin-dep...
activation of...
regulation of...
negative regulation of peptidase activity
regulation of tyrosine...
glycoprotein...
phagocytosis
apical pro...
adhes...
egg coat formation
organ or tissue specific...
pallium development
gliogenesis
neutrophil homeostasis
mucosal immune...
chaeta development
sensory organ...
cluster...
parturition
very-low-de...
placenta developm...
molting cycle, collagen and...
maintenance...
smooth muscle tissue...
ant...
tRNA 3'-end process...
allantoin metabo...
cell...
calc...
O-glyca...
sulfur amino acid...
acetald...
glucoco...
alkanesulf...
fucosylati...
N-glycan fucosylati...
lipoprotein metabolic process
lipoprotein biosynthetic process
ketone catabolic process
phyllo...
tauri...
vitamin B6 metabolic process
pyridoxa...
L-cysteine metabolic...
protein neddyla...
brexanolo...
brexanolo...
ter...
cell...
negative...
pyroptosis
negative regulation of protein-...
extrinsic apoptotic signaling...
regulation of microvill...
extracell...
olefinic compound biosynth...
regulati...
negat...
regula...
regulati...
negati...
reg...
regulati...
regul...
positive regulatio...
positive regulatio...
regulation of protein...
regul...
regulation of heterotyp...
regulation of protei...
regulation of protein polyubiqu...
gangli...
sesq...
isoprenoid metabolic process
puri...
purine deoxyri...
xanthine metabolic process
sesquit...
purine deoxyrib...

Figure 4

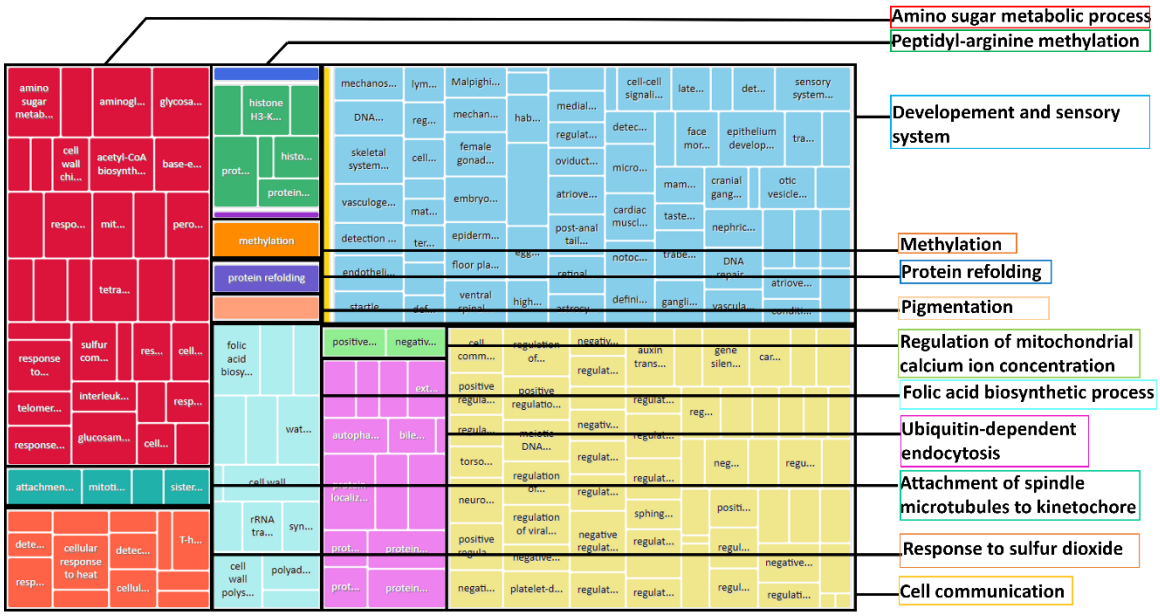
Amino sugar metabolic process
Peptidyl-arginine methylation
Developement and sensory system
Methylation
Protein refolding
Pigmentation
Regulation of mitochondrial calcium ion concentration
Folic acid biosynthetic process
Ubiquitin-dependent endocytosis
Attachment of spindle microtubules to kinetochore
Response to sulfur dioxide
Cell communication

Figure 5

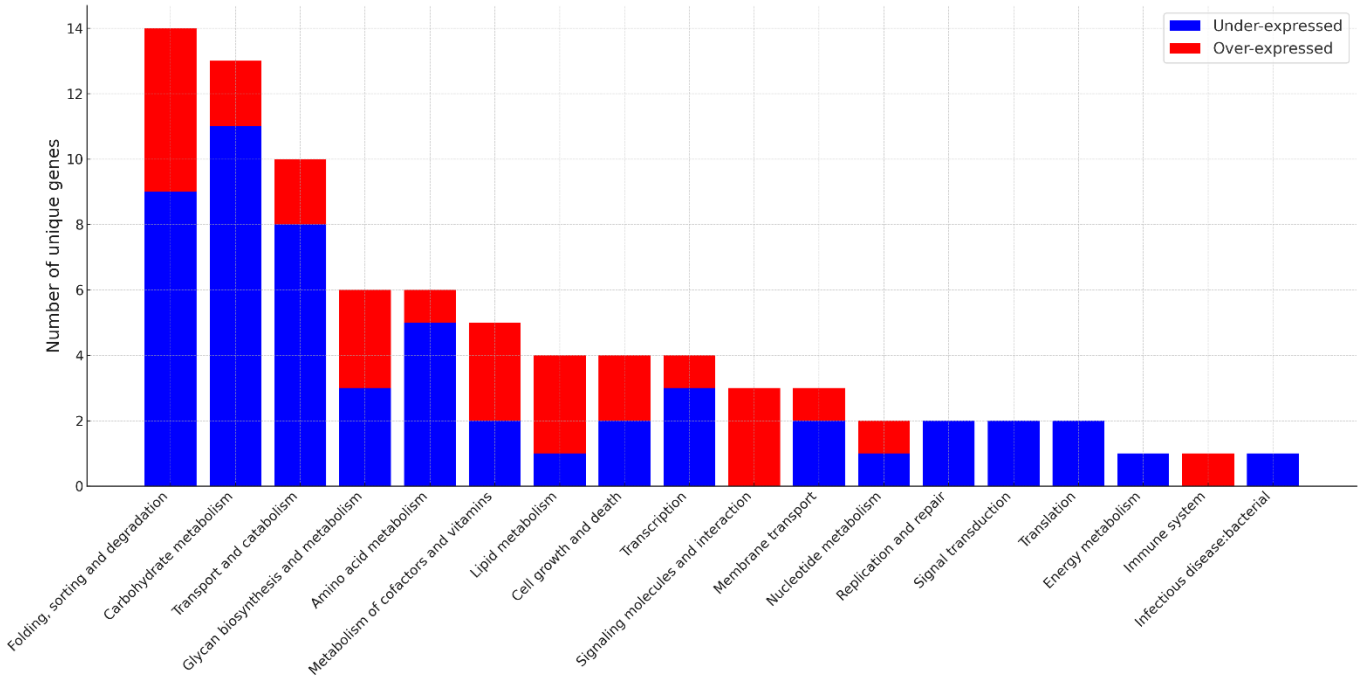
Under-expressed
Over-expressed
Number of unique genes
0
2
4
6
8
10
12
14
Folding, sorting and degradation
Carbohydrate metabolism
Transport and catabolism
Glycan biosynthesis and metabolism
Amino acid metabolism
Metabolism of cofactors and vitamins
Lipid metabolism
Cell growth and death
Transcription
Signaling molecules and interaction
Membrane transport
Nucleotide metabolism
Replication and repair
Signal transduction
Translation
Energy metabolism
Immune system
Infectious disease:bacterial

Figure 6

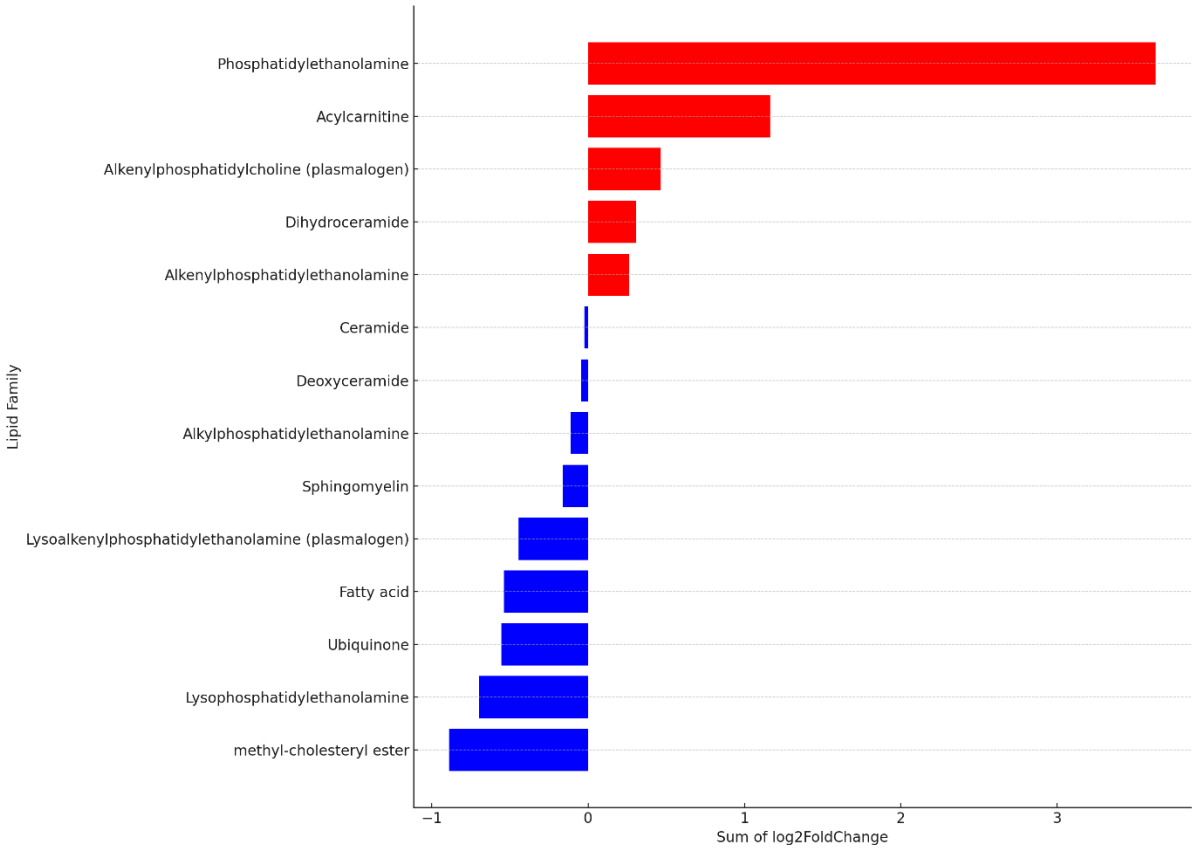
Phosphatidylethanolamine
Acylcarnitine
Alkenylphosphatidylcholine (plasmalogen)
Dihydroceramide
Alkenylphosphatidylethanolamine
Ceramide
Deoxyceramide
Alkylphosphatidylethanolamine
Sphingomyelin
Lysoalkenylphosphatidylethanolamine (plasmalogen)
Fatty acid
Ubiquinone
Lysophosphatidylethanolamine
methyl-cholesteryl ester
Lipid Family
−1
0
1
2
3
Sum of log2FoldChange